UAS Flexible Configuration for Optimum Performance in ISTAR Military Missions

Cătălin CIOACĂ[1]*, Vasile Florin POPESCU[2], Vasile PRISACARIU[1], Sebastian POP[1], Cristian VIDAN[3]

[1] "Henri Coandă" Air Force Academy, Faculty of Aeronautical Management, Brasov, Romania
catalin.cioaca@afahc.ro (**Corresponding author*), vasile.prisacariu@afahc.ro, sebastian.pop@afahc.ro

[2] "Carol I" National Defence University, Faculty of Security and Defence, Bucharest, Romania
popescuveve@gmail.com

[3] "Ferdinand I" Military Technical Academy, SATAS Centre of Excellence, Bucharest, Romania
vidan.cristian@yahoo.com

Abstract: The main purpose of this paper is to present a pilot configuration management system, namely QuadFlexArch, necessary for the planning of ISTAR military missions performed with unmanned aerial systems (UASs). The creation of this system started due to an operational need identified during the modernization of the Phoenix 30 quad-rotor vertical take-off and landing (VTOL) UAS. QuadFlexArch has been designed so as to allow being constantly updated according to the most recent operational requirements, associated with the latest UASs, but also with the new validated and available technical solutions. The model adopted for the design and development of the configuration management system allows the identification and evaluation of UAS by testing the key performance parameters (the noise level, thrust, torque, power, speed for the motor-propeller assembly, ESC signal and the reconfiguration time for a certain mission), the determination of the flight autonomy and data integration into a decision support platform designed in the Delphi programming language. The obtained result is in the form of a hierarchy of technical solutions available for optimal mission planning.

Keywords: Unmanned aerial system, Key performance indicators, Configuration management, Decision-making platform.

1. Introduction

In the context of the proliferation of conventional and unconventional threats in the military operational environment, there is an extensive process of acquiring military equipment and weapons that creates additional pressure on the human factor to achieve the highest capability level as soon as possible. UASs are already positioned on the transition curve as validated systems. They are the direct beneficiaries of the technological progress from the last period.

Low costs, flexibility and modularity, low risk for the human factor, but especially the advantages granted by the possibility of procuring data from hard-to-reach environments and providing them in real time, accurately, to decision makers and action structures, have produced a revolution in planning and conducting military actions.

This new military capability must meet dynamic operational requirements, supporting with Imagery Intelligence (IMINT) information the military structures that perform the full range of operations on the ground, and in the airborne and maritime environments, independently, or in a joint or combined manner, through research and aerial observation, day and night.

UASs are already successfully performing a variety of military missions: intelligence, surveillance, target acquisition, and reconnaissance (ISTAR), combat (air-to-air, air-to-ground), multi-purpose, radar and communication relay, materials delivery and supply. ISTAR is a system that uses UASs to collect and transmit real-time information about enemy/terrain (Udeanu, Dobrescu & Oltean, 2016). ISTAR missions are high-risk operations conducted in a hostile environment. Phoenix 30, specialized in ISTAR missions, is a quad-rotor vertical take-off and landing (VTOL) UAS, capable of flying to fixed point or evolving at low speed in a three-dimensional space. It became part of the equipment of the Romanian army approximately 6 years as go (sUAS News, 2016), being at the end of its operational life cycle. The ongoing modernization process includes, in addition to the replacement of equipment suffering from physical and functional obsolescence, a flexible approach to architectural management in accordance with the new mission requirements.

The analysis of the operational requirements for the use of Phoenix 30 in ISTAR missions highlights the following key performance indicators: noise level, autonomy and a configuration time for a new mission.

https://doi.org/10.24846/v31i3y202211

The literature allocates an ample space to technical and procedural solutions for reducing the noise produced by propellers of civilian drones: modification of propellers according to the owl biological model to reduce sound pressure level (SPL) (Callender, 2017); modification of the geometry (Wisniewski et al., 2015) or the upper surface of the propellers (Clark et al., 2015); active noise cancellation using an external anti-noise signal (Narine, 2020); managing the noise level by applying operating restrictions (Torija & Clark, 2021).

If for the civilian use the noise pollution produced by drones flying at altitudes lower than 120 m is being regulated (European Union Aviation Safety Agency, 2020), for the military field the requirement is that this level be lower than the noise of the battlefield, so that it cannot be detected.

The increasing noise pollution produced by civilian drones is already felt in public spaces, but it is considered that it will increasingly affect the fauna as well, becoming a difficult problem to manage at the European level (European Parliament, 2019).

Knowing the noise level according to the operational procedures is essential for the civil field from the perspective of legislation and standardization (American National Standards Institute, 2020), and for the military field from the perspective of achieving/countering surprise.

Autonomy, in operational terms, is analyzed as a function of the distance to the area to be researched, the cruising altitude and speed, and in technical terms, it becomes a function of the parameters of the propulsion system (thrust, torque, power and speed). Rotors are electric propulsion units (EPUs) consisting of a fixed-pitch propeller, brushless DC (BLDC) motor and an electronic speed controller (ESC) (Nedeoglo et al., 2017).

Configuration time for the new mission is an important indicator for the beneficiary which was not yet explored in the literature, but is justified by the time constraints that characterize military missions. This indicator includes the time for mission data analysis, the loading of mission data on the decision support platform, the implementation of the optimal solution and the calibration of the system for the new mission.

The modular architecture approach presents the advantages of diversifying the type of mission and improving performance indicators (Seo, Paik & Yim, 2019; Saldana et al., 2018). This research solves some of these challenges, in the sense of designing an interactive tool that, depending on operational requirements, by exploiting a database, prioritizes the available configuration solutions (propeller - engine) for better mission planning. The initial data was obtained for three types of engines and three types of propellers, using the RC Benchmark Series 1580 test stand. The database resulting from the testing process is operated by a decision support platform (QuadFlexArch) developed with the Delphi 7 programming language.

The paper is innovative and can be considered relevant for the research field of military UASs for the following reasons:

- testing the performance of the motor-propeller assembly in different configurations under laboratory conditions;
- the development for the first time of a database that includes the key technical parameters specific to multicopter UASs with military use;
- the innovative design of an interactive tool capable of improving the military decision-making process by running a database.

The paper is organized as follows. Section 2 presents the method and test equipment employed for collecting specific traction and noise data. Section 3 puts forth the proposed decision support platform and the details of its architecture are described. Section 4 includes the conclusions and summarizes the main results obtained during the analysis that was carried out.

2. Test Equipment and Method

2.1 Thrust Stand, Electric Motors, and Propeller Blades

A RC Benchmark Series 1580 digital thrust stand was used for collecting specific traction data (Figure 1(a)), and Optical RPM Probe V2.2 was used for accurately measuring rotor speed. The method used for controlling the motors is based on the direct connection between the test stand and the computer via USB and the use of software

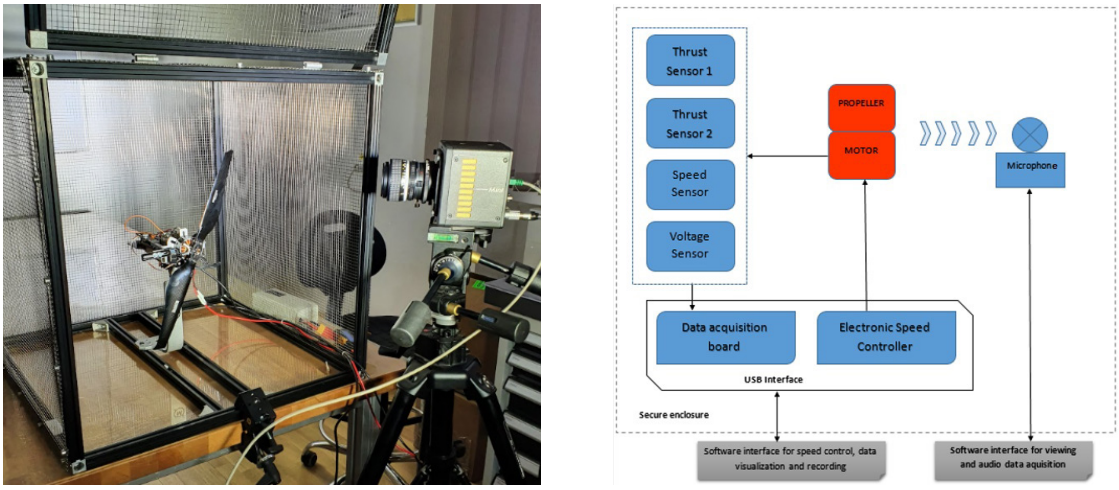

(a) (b)

Figure 1. Thrust Stand
(a) RC benchmark Series 1580 thrust stand and motor with propeller installed
(b) Functional Diagram

for automatic control and data recording. ESC was manually controlled using the user scripting interface. Engine and propeller data were viewed in real time, and at the end of each scheduled test, they were exported to a .CSV file (Figure 1(b)).

Three types of motors were tested: T-Motor MN4014 rated at 400 KV, T-Motor MN5008 rated at 400 KV and T-Motor MN4006 rated at 380 KV. A 22,000 mAh battery, 22.2 V, 6 cells, Lithium polymer (Li-Po) provided power to the motors. The carbon fiber propellers, namely the EOLO propeller - 15x5.5 inch, the folding propeller - 15x5 inch and the O15 propeller - 15x5 inch, with two blades and fixed pitch were tested counterclockwise (two clockwise).

2.2 Method and Results

ESC, various motor-propeller combinations and the battery were successively installed on the digital thrust support. Digital support was connected via USB to a laptop running RC Reference Software. The rotor speed was increased in steps by 1000 µs ESC signal in a range between 1000 µs and 2000 µs, and the speed stabilization time before measurement was set to 5 seconds. The process was repeated 5 times for each available propeller combination. The data was collected continuously and saved in a special file.

Noise level testing for each propeller configuration was performed by positioning a datalogger at the rear of the RC Benchmark traction bracket on which the engine and propeller were mounted, 30 cm from the propeller. The distance to the propeller was set so that the datalogger was inside the protection grid of the test bench, and the different positioning of the datalogger followed a circle with a radius of 15 cm from the rotor shaft, according to flow field visualization in ascending smoke conditions (Figure 2).

Figure 2. Flow field visualization in ascending smoke conditions

The raw thrust data collected by the RC Benchmark traction support was transferred from the RC Benchmark software to Excel, with the help of which the graphs corresponding to the area of interest were created: 60% to 100% of the engine rotation frequency. The graphs represent the evolution of the thrust, electrical motor speed and noise parameters for the MN4014 T-Motor and the

three types of propellers mentioned in subsection 2.1 (Figure 3), and experimental data for these propellers is included in Tables 1, 2 and 3.

The analysis of the data obtained from the tests highlights, on the one hand, the direct relationship between electrical motor speed and thrust, and on the other hand, the direct relationship between them and the noise level for the folding propeller, and the inverse relationship for the EOLO and O15 propellers, respectively. At the speed values corresponding to the area of interest for the EOLO

Table 1. Experimental data for the EOLO propeller and MN4014 motor

ESC signal (µs)	Torque (N·m)	Thrust (gf)	Voltage (V)	Current (A)	Electrical Motor Speed RPM)	Noise (dB)
1500	0.1850	956.5029	24.03	4.85	9751	74.8
1600	0.2600	1,345.6460	23.82	7.62	9738	77.5
1700	0.3479	1,805.7886	23.54	11.54	11150	71.5
1800	0.4443	2,303.9737	23.17	16.52	12481	69.1
1900	0.5493	2,833.1454	22.74	22.76	13730	64.2
2000	0.5750	2,964.2032	22.48	24.82	14023	62

Table 2. Experimental data for the O15 propeller and MN4014 motor

ESC signal (µs)	Torque (N·m)	Thrust (gf)	Voltage (V)	Current (A)	Electrical Motor Speed (RPM)	Noise (dB)
1500	0.1742	922.8823	24.46	4.68	9311	64.6
1600	0.2397	1,286.0421	24.28	7.22	10069	69.8
1700	0.3151	1,707.5721	23.97	10.59	11528	69.8
1800	0.4004	2,175.1633	23.59	15.20	13063	63.9
1900	0.4865	2,668.8523	23.16	20.54	14405	61.5
2000	0.5183	2,836.2139	22.98	22.38	14734	57.4

Table 3. Experimental data for the folding propeller and MN4014 motor

ESC signal (µs)	Torque (N·m)	Thrust (gf)	Voltage (V)	Current (A)	Electrical Motor Speed (RPM)	Noise (dB)
1500	0.1654	927.1674	24.89	4.53	9104	75.86
1600	0.2255	1,271.8148	24.79	6.84	10438	79.92
1700	0.2994	1,706.4542	24.64	10.11	12002	84.95
1800	0.3871	2,216.8525	24.46	14.66	13661	87.98
1900	0.4783	2,731.0335	24.25	20.25	15149	91.02
2000	0.5068	2,892.7154	24.13	22.11	15594	92.77

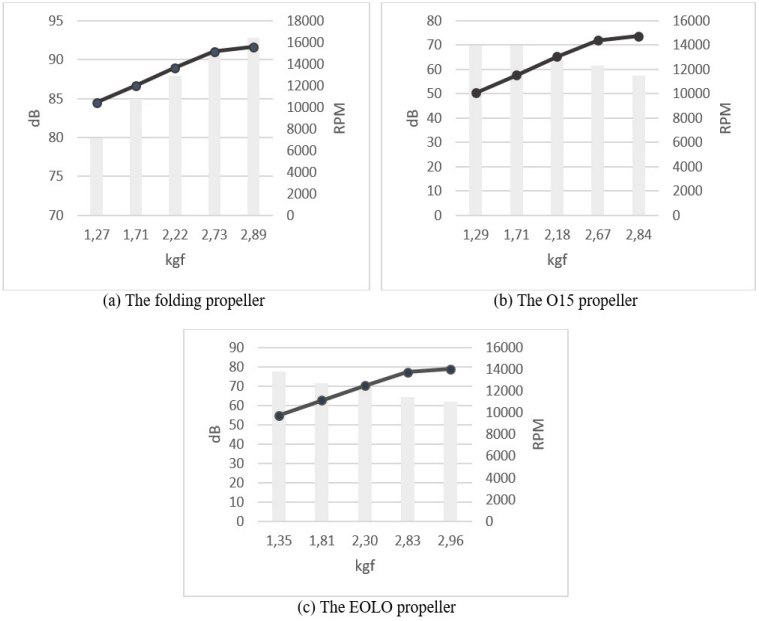

(a) The folding propeller

(b) The O15 propeller

(c) The EOLO propeller

Figure 3. Thrust, noise and electrical motor speed for the MN4014 motor for the same ESC signal

and O15 propellers, although the rate of decrease for the noise level is similar (approx. 20%), the range of values for the EOLO propeller is higher than that for the O15 propeller (Figure 3(b), (c)). For the folding propeller, the rate of noise level increases by 15%, and the lower limit of the range of values exceeds the maximum level corresponding to the other types of propellers (Figure 3(a)).

3. Decision-Making Platform

3.1 Theoretical Highlights

In order to substantiate the software tool used in the decision-making process, it is necessary to reveal some theoretical aspects regarding the equations underlying the logical and numerical codes.

A. Flight time (t_f) is defined (Anon, 2022) as a function of battery capacity (Q) and the current consumed by all equipment during flight (I_{fl}) (equation 1).

$$t_f = \frac{\frac{Q}{1000}}{I_{fl}} \cdot 60 \tag{1}$$

The total current consumed during flight is defined as a function of the flight load (L_f), which depends on the type of flight and the total mass of the multicopter (equation 2).

$$I_{fl} = I_{\max fl} \cdot L_f \tag{2}$$

Also, the number of batteries required by equation (3) is determined, where (C) represents the discharge rate for the batteries.

$$N_b = \left[\frac{I_{\max fl}}{\frac{Q \cdot C}{1000}} \right] \tag{3}$$

B. The static thrust (P) transmitted by the motors to the propeller is determined using equation (4), where (p_c) is a constant of the propeller and n is the speed (in RPM) (Dickey, 2022).

$$P = p_c \cdot n^{3,2} \tag{4}$$

The mass can be expressed (from $F = m \cdot a$) using equation (5), where (D) represents the diameter of the propeller, ρ the density of the air, and g the gravitational acceleration.

$$m = \frac{\left[\frac{\pi}{2} \cdot D^2 \cdot \rho \cdot P^2 \right]^{\frac{1}{3}}}{g} \tag{5}$$

A slightly oversized static thrust of the motors leads to a higher theoretical value of the payload.

3.2 QuadFlexArch Application

The decision-making process is based on a software tool made in the Delphi programming language, this software is based on decision optimization for logistics solutions according to atmospheric and operational requirements. The graphical user interface (GUI) provides three tabs: a tab for entering and validating data, a tab for results and data export, and a tab for instructions for use (Figure 4).

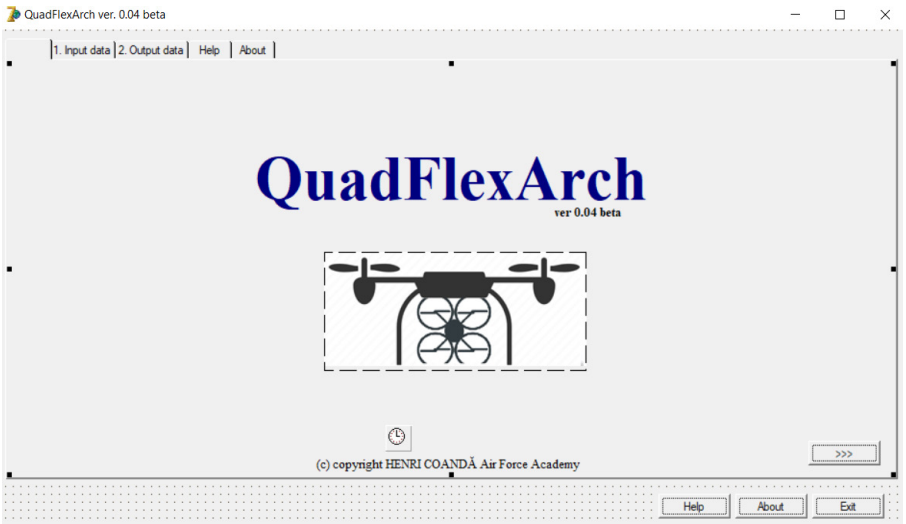

Figure 4. QuadFlexArch Interface Screenshot – GUI

The input data offers the possibility to choose among three generic missions (IMINT, transport and hybrid missions), target data (distance and temperature), as well as operational data: noise level generated, time of flight readiness, speed and traction of the chosen propulsion system and theoretical range expressed as a percentage.

A data reset command was entered to reset the edit fields. Data editing fields benefit from the hint function for indicating valid data ranges. Running the code on the input tab provides an option for the UAS solution along with an exportable text report (Figure 5).

The time available for mission preparation determines the three configuration possibilities of the UAS: default, change propellers, change propellers and motors. The maximum noise level allowed for a certain mission type determines the propeller configuration.

The output tab provides data on how to set the drone (default status, propeller and motor settings), along with the calculated flight parameters (distance, range of operations and flight autonomy). The software interface also provides an option for exporting data for later use (Figure 6).

The flight autonomy calculated for the UAS configuration-solution is compared with the operational flight requirements, and the result indicates one of the two possible decisions: start mission or mission hold. The *Mission Hold* indicator is interpreted in terms of re-planning the position of the ISTAR mission starting point. The *Help* tab provides a series of instructions for using the software tool.

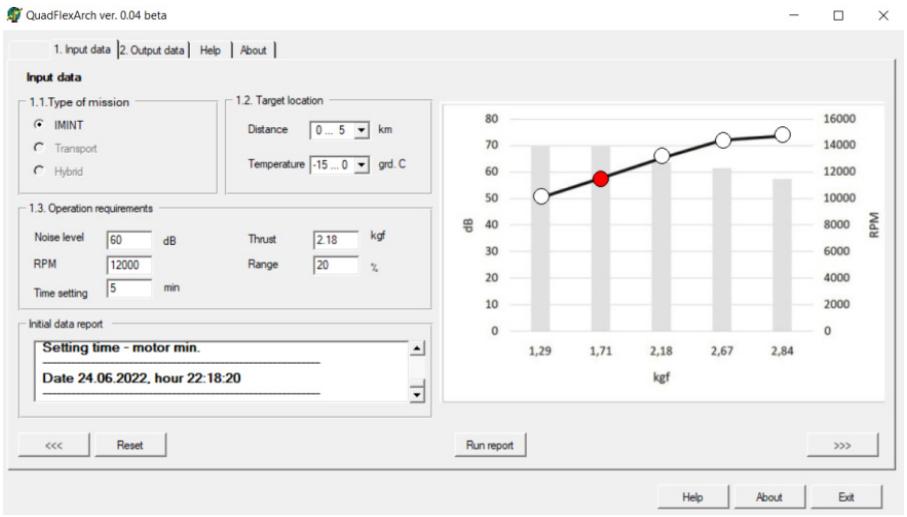

Figure 5. Input data platform architecture

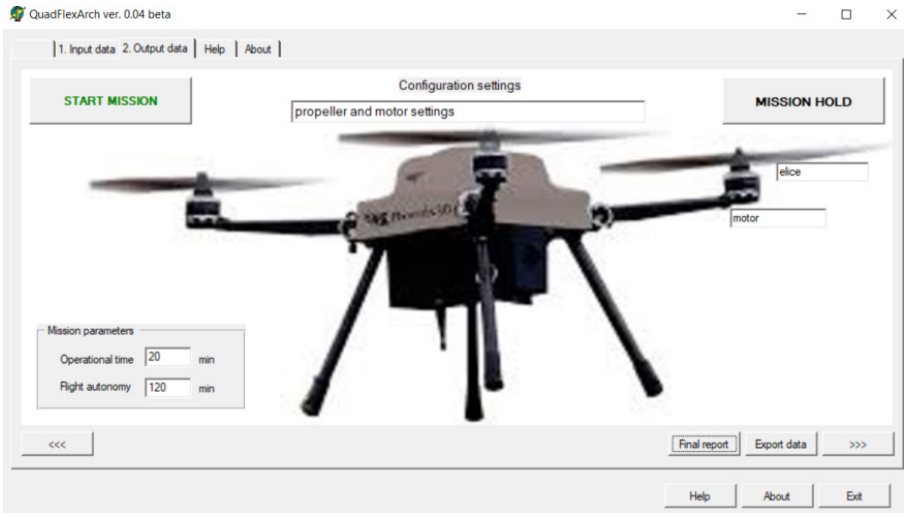

Figure 6. Output data platform architecture

4. Discussion and Conclusion

This paper presented the preliminary results of the performance tests for the motor-propeller assembly. Currently there are no such databases for research purposes. The experiments were performed on several types of available propellers and engines, which were compatible with the UAS Phoenix 30 model.

The research becomes particularly important in the following context: when tested at the settings corresponding to the operational requirements, some parts of the equipment do not behave according to the quality specifications of the manufacturer (e.g. the folding propeller is presented as being low noise, and the results show that it is the noisiest of the three variants tested), and other parts of the equipment can be replaced, thereby obtaining a superior performance (e.g. the noise performance of the O15 propeller is superior to that of the EOLO propeller).

The obtained results correspond to the operational requirements for using the drone in ISTAR missions. Due to the modular functional architecture of the drones and to the accelerated technological progress, the performance of these systems can be improved/optimized without the need to replace the entire system.

The list of mission needs is constantly updated, and operational requirements are constantly evolving. The advantages that these systems offer

(a state-of-the-art technology, affordable prices, minimal risks) do not justify the acquisition-based approach, but rather the modularity-based approach and an efficient configuration management.

The decision support platform integrated with the command-control system has been designed in a flexible way to meet future operational requirements, both for the Phoenix 30 model and for other autonomous rotary wing aerial systems that could be developed/ purchased.

The configuration management system is designed to allow the easy integration of new data platforms associated with new types of UASs that became part of the equipment of the Romanian army, with new types of missions and available technological developments.

Acknowledgements

The research presented in this article has been funded by the Ministry of Investments and European Projects through the Human Capital Sectoral Operational Program 2014-2020, Contract no. 62461/03.06.2022, SMIS code 153735.

REFERENCES

American National Standards Institute (2020). *Standardization Roadmap for Unmanned Aircraft Systems, Version 2.0.*, Available at: <https://share.ansi.org/Shared%20Documents/Standards%20Activities/UASSC/ANSI_UASSC_Roadmap_V2_June_2020.pdf>.

Anon (2022). *Drone LiPo Battery Calculator*. Available at: <https://www.translatorscafe.com/unit-converter/en-US/calculator/multicopter-lipo-battery>.

Callender, M. N. (2017). UAS Propeller/Rotor Sound Pressure Level Reduction Through Leading Edge Modification. *Journal of Applied Mechanical Engineering*, *6*, 254.

Clark, I. A., Alexander, W. N., Devenport, W., Glegg, S., Jaworski, J. W., Daly, C. & Peake, N. (2015). Bio-Inspired Trailing Edge Noise Control. In *Proceedings of the 21st AIAA/CEAS Aeroacoustics Conference*, DOI:10.2514/6.2015-2365.

Dickey, J. (2022). *Static Thrust Calculation*. Available at: <https://quadcopterproject.wordpress.com/static-thrust-calculation>.

European Parliament (2019). *Civil and military drones. Navigating a disruptive and dynamic technological ecosystem*. Available at: <https://www.europarl.europa.eu/RegData/etudes/BRIE/2019/642230/EPRS_BRI(2019)642230_EN.pdf>.

European Union Aviation Safety Agency (2020). *What Are the Requirements under the Subcategories of the 'Open' Category?* Available at: <https://www.easa.europa.eu/ faq/116452>.

Narine, M. (2020). *Active Noise Cancellation of Drone Propeller Noise through Waveform Approximation and Pitch-Shifting*. Computer Science Thesis. Available at: <https://scholarworks.gsu.edu/cgi/viewcontent.cgi?article=1102&context=cs_theses>.

Nedeoglo, N., Rotaru, C., Danici, A., Seinic, V., Sprincean, V., Vozian, C., Cazan, V., Corcimari, I. & Cebotaru, E. (2017). In Coord. Daponte, P., Paladi, F. & Bulimaga, T. (Eds.), *Educație pentru drone*. *Note de curs*, Moldova State University, Chisinau.

Saldana, D., Gabrch, B., Li, G., Yim, M. & Kumar, V. (2018). ModQuad: the flying modular structure that self-assembles in midair. In *2018 IEEE International Conference on Robotics and Automation*. DOI: 10.1109/ICRA.2018.8461014.

Seo, J., Paik, J., & Yim, M. (2019). Modular Reconfigurable Robotics, *Annual Review of Control, Robotics, and Autonomous Systems, 2*, 63-88.

sUAS News (2016). *UAV Solutions, Inc. Deliver four Phoenix 30 UAS to Romania*. Available at: <https://www.suasnews.com/2016/01/uav-solutions-inc-deliver-four-phoenix-30-uas-to-romania/>.

Torija, A. J. & Clark, C. (2021). A Psychoacoustic Approach to Building Knowledge about Human Response to Noise of Unmanned Aerial Vehicles, *International Journal of Environmental Research and Public Health*, *18*(2), 682.

Udeanu, G., Dobrescu, A. & Oltean, M. (2016). Unmanned Aerial Vehicle In Military Operations. In *Proceedings of the 18th International Conference on Scientific Research and Education in the Air Force – AFASES* 2016 (pp. 199-206).

Wisniewski, C., Byerley, A., Heiser, W. H., Van Treuren, K. W. & Liller, T (2015). The Influence of Airfoil Shape, Reynolds Number and Chord Length on Small Propeller Performance and Noise. In *Proceedings of the 33rd AIAA Applied Aerodynamics Conference*. DOI:10.2514/6.2015-2266